



Published in final edited form as:

J Nat Prod. 2015 March 27; 78(3): 441–452. doi:10.1021/np500840n.

Biosynthetic Products from a Nearshore-Derived Gram-Negative Bacterium Enable Reassessment of the Kailuin Depsipeptides

Christine M. Theodore[†], Nicholas Lorig-Roach[†], Patrick C. Still[†], Tyler A. Johnson[†], Marija Drašković[†], Joshua A. Schwochert[†], Cassandra N. Naphe[†], Mitchell S. Crews[†], Simone A. Barker[†], Frederick A. Valeriote[‡], R. Scott Lokey[†], and Phillip Crews^{*,†}

[†]Department of Chemistry and Biochemistry, University of California, Santa Cruz, California 95064, United States

[‡]Josephine Ford Cancer Center, Henry Ford Health System, Detroit, Michigan 48202, United States

Abstract

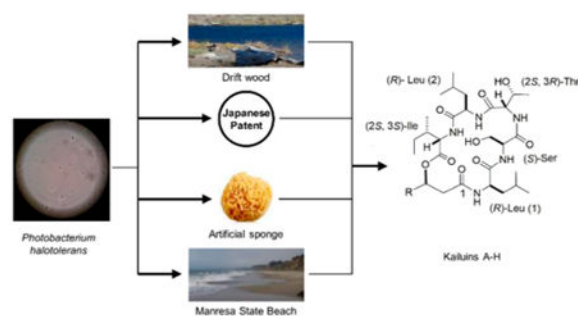
Sampling of California nearshore sediments resulted in the isolation of a Gram-negative bacterium, *Photobacterium halotolerans*, capable of producing unusual biosynthetic products. Liquid culture in artificial seawater-based media provided cyclic depsipeptides including four known compounds, kailuins B–E (**2–5**), and two new analogues, kailuins G and H (**7** and **8**). The structures of the new and known compounds were confirmed through extensive spectroscopic and Marfey's analyses. During the course of these studies, a correction was made to the previously reported double-bond geometry of kailuin D (**4**). Additionally, through the application of a combination of derivatization with Mosher's reagent and extensive ¹³C NMR shift analysis, the previously unassigned chiral center at position C-3 of the β -acyloxy group of all compounds was determined. To evaluate bioactivity and structure–activity relationships, the kailuin core (**13**) and kailuin lactam (**14**) were prepared by chiral synthesis using an Fmoc solid-phase peptide strategy followed by solution-phase cyclization. All isolated compounds and synthetic cores were assayed for solid tumor cell cytotoxicity and showed only minimal activity, contrary to other published reports. Additional phenotypic screenings were done on **4** and **5**, with little evidence of activity.

*Corresponding Author: Tel: (831) 459-2603. Fax: (831) 459-2935. pcrews@ucsc.edu.

Supporting Information: The Supporting Information contains a selective view of biosynthetic products from marine-derived strains of Gram-negative bacteria, NMR spectra, detailed explanations of Marfey's analysis and chromatographic optimizations, and information on synthetic methodologies. This material is available free of charge via the Internet at <http://pubs.acs.org>.

Notes: The authors declare no competing financial interest.

Dedication: Dedicated to Dr. William Fenical of Scripps Institution of Oceanography, University of California–San Diego, for his pioneering work on bioactive natural products.



A shift in the focus for the study of marine biosynthetic products appears to be under way. This change involves an emphasis on compounds isolated from culturable heterotrophic microorganisms rather than from marine invertebrates (sponges, cnidarians, and tunicates). It is clear that the ocean environment represents a vast resource for obtaining new chemical entities from bacteria and fungi. In fact, recent estimates indicate more than 10^5 microorganisms could exist.¹ Foreshadowing this swing to marine microorganisms was a 1993 review published by Fenical² entitled “Chemical Studies of Marine Bacteria: Developing a New Resource”. This work summarized some 50 biosynthetic products derived from oceanic bacteria and has been highly cited by others [ca. 270 times, Web of Science]. As a measure of recent progress, 119 novel natural products from the culturing of marine bacteria were reported during the 2012 calendar year.^{3–5} A majority of the microorganisms were Gram-positive species.

One motivation for the project described herein was our conclusion that the study of products from marine-derived Gram-negative bacteria remains underexplored. The diversity of culturable heterotrophic bacteria in seawater, while incompletely understood,⁶ is thought to be dominated by Gram-negative rods, mainly of the phylum Proteobacteria. Some examples of well-known genera within this group include *Vibrio*, *Pseudoalteromonas*, and *Pseudomonas*. Yet, the tally of natural products from this assemblage is relatively small. Additionally, while members of the α -Proteobacteria seem to be the most abundant, it is the γ -Proteobacteria that appear to be most successfully cultured.⁷ Gaining command of the literature linking biosynthetic products to their various Gram-negative sources was accomplished at the outset of our project. This involved building a small database of 63 lead molecular structures (shown in Figure S1, Supporting Information) using results from four of the six major classes of the Proteobacteria (the other two remain unstudied). Also evident to others and ourselves is that many sponge metabolite scaffolds have parallel or identical features to those isolated from terrestrial-derived Gram-negative bacteria, especially myxobacteria (δ -Proteobacteria).^{8–10}

The initial goal of this project was to develop a library of California coastal zone-derived Gram-negative strains to seed subsequent metabolite studies. Our hypothesis was that processing fresh environmental samples using baiting techniques designed to maximize isolation of δ -Proteobacteria would yield enhanced strain diversity. However, large numbers of rapidly growing Gram-negative cultures were observed that were γ -Proteobacteria, and only a few had the characteristics expected from the δ -class. Specific details of these biological outcomes, including an overview of the strains and their diversity, will be

published elsewhere. This account reports on an initial success in the saltwater culturing of a nearshore γ -Proteobacteria species characterized as *Photobacterium halotolerans* (M128SB283Ax), which produces six cyclic depsipeptides of the kailuin family (2–5, 7, and 8) including two new analogues (7 and 8).

Results and Discussion

The early reports of metabolites from Gram-negative marine bacterial strains involved the pursuit of samples obtained from seawater.² This strategy continues to be successful. For example, the antitumor cyclic depsipeptide didemnin B (originally from Caribbean tunicates) was recently reisolated through the culturing of *Tistrella* sp. (α -Proteobacteria, Figure S1, Supporting Information), obtained from an Indo-Pacific water column sample.^{5,11} The current work began by collecting sediments from 41 beaches in the Monterey Bay, CA, region. A total of 820 distinct samples yielded 54 cultivable strains thus far. The strain isolation step involved baiting with *Escherichia coli* streaks on nutrient-deficient agar.¹² Each strain was later examined using 16S rRNA sequences, and the majority (59%) could be classified as members of the phylum Proteobacteria; most proved to be γ -Proteobacteria.

The campaign to identify the top chemically prolific strains from the isolates described above involved subjecting dichloromethane (CH₂Cl₂) extracts of selected small-scale cultures (5 L) to metabolite profiling via LC/MS-ELSD. Since this operation was done prior to the completion of molecular taxonomic analysis, the initial prioritizations for advanced chemical study relied on mass spectrometric results. Thus, attention was drawn to one sample displaying intense m/z ions (726, 740, 752, 754 [M + H]⁺) for several chromatographic peaks that were not seen in other cultures. This strain, coded M128SB283Ax, was derived from sediment obtained at Manresa State Beach, CA, and subsequently identified as *Photobacterium halotolerans*.

The next step involved cross referencing the initial mass spectrometric data described above to the formulas and structures known from prior study of the *Photobacterium* cultures. Even though *Photobacterium* is often associated with disease states in a number of marine organisms,¹³ the literature on its biosynthetic products is relatively scant. Representative examples are shown in Figure 1. Some highlights from this compilation are (a) only four defined species of the genera have been explored chemically including *P. angustum*, *P. damsela*, *P. halotolerans*, and *P. phosphoreum*; (b) no compound isolated from *Photobacterium* cultures matched the MS m/z data observed; and (c) cyclic depsipeptides dominate the list, indicating dereplication efforts should emphasize this class.

As the project progressed, strain M128SB283Ax was firmly characterized through repeated 16S rRNA analysis. It showed 98% likeness to the *P. halotolerans* type specimen (MACL01), which is above the cutoff value for bacterial species similarity identification.²³ This identification was further validated by follow-up examination using the *recA* and *rpoA* genes²⁴ (P. Dunlap, unpublished results using our sample). As an interesting biological circumstance, *P. halotolerans* was first reported in 2006 from water samples gathered in Lake Martel, a subterranean saline environment in Mallorca, Spain.²⁴ At the time of the

2006 report, there were 12 defined *Photobacterium* species. Subsequently, this group has now grown to include 29 members, including a few previously assigned to the genus *Vibrio*. Figure 2 depicts strain M128SB283Ax phylogeny in a maximum likelihood tree, with *P. halotolerans* forming a branch alongside *P. ganghwense*, which has not yet been a subject of natural products study (Figure 1). Many *Photobacterium* species live in association through mutual and pathogenic relationships with marine organisms. Consequently, they can be difficult to isolate. The present finding represents the first example of the isolation and chemical study of any *Photobacterium* species from California coastal zone sediment and suggests that its members could be more widespread than previously believed.

The gateway to the isolation and analysis of the secondary metabolites from strain M128SB283Ax involved the scale-up culture and purification outlined in Scheme 1. Exhaustive extraction of the culture broths (16 L) provided an oil, which was then subjected to solvent partitioning. This afforded 0.45 g of a CH₂Cl₂-soluble fraction and 1.2 g of water-soluble material. The CH₂Cl₂ material was subjected to a preparative HPLC step gradient²⁵ to provide six prefractions (F0 was discarded). The fractions F3–F5 contained several compounds with mass spectrometric [M + H]⁺ *m/z* values ranging from 726 to 754. These were pooled, and their constituents were further separated by HPLC. Six pure compounds were isolated from the 12 fractions collected, and six were pursued further including H2 (0.8 mg), H3 (2.0 mg), H4 (3.2 mg), H6 (1.7 mg), H9 (1.7 mg), and H10 (4.0 mg).

A metabolite in fraction H4 served as the lead for dereplication. The molecular formula was established from high-accuracy mass spectrometry (HAMS) as C₃₉H₆₉N₅O₉, based on *m/z* [M + K]⁺ 790.4739. A literature search on this molecular formula yielded only one natural product hit, (+)-kailuin D (**4**),²⁶ shown in Figure 3. The ¹H and ¹³C NMR data (shown in Table 1; see also Figures S2–S8, Supporting Information) confirmed the match. A 1997 report on the structure of kailuin D employed liquid culture of a bacterium identified provisionally as in the genus *Vibrio* and obtained from driftwood in Hawaii. Also, three other analogues, (+)-kailuins A–C (**1–3**), were reported from this culture broth. Added to this list, shown in Figure 3, are two other analogues as follows. Kailuin E (**5**) was isolated from a culture sample identified as a *Vibrio* sp. (marine environmental source not stated)²⁷ and kailuin F (**6**), obtained from a *Vibrio* sp. cultured from the surface of an artificial cellulose sponge deployed for 1 h at –10 m in Okinawa.²⁸

On close inspection, uncertainties arose pertaining to the properties of the compound from fraction H4 compared to those published for kailuin D (**4**). First, the NMR data shown here were consistent with the presence and sequence of the five amino acids and acyloxy substructures in **4**, but the optical rotation measured ([α]_D –15.0, *c* 0.8, MeOH) was not in agreement with the published value ([α]_D +9.5, *c* 1.0 MeOH).²⁶ Second, the Marfey's analysis published on **4** did not distinguish between the possibilities of (2*S*,3*R*)-Thr, vs (2*S*,3*S*)-Thr.²⁹ Third, the ¹³C NMR data listed for the allylic carbons at C-6 (δ_C 26.6) and C-9 (δ_C 27.6) were consistent with a *Z* rather than the *E* geometry reported.³⁰ Finally, the absolute configuration at the β-acyloxy position was not defined, but *R* configurations had been reported for this same residue in related compounds, solonamide A and unnarmicin A (Figure 1). Despite lacking original samples from previously published reports, the immediate next steps were to resolve all of these issues.

A multistep process was used to reinvestigate the total structure of kailuin D (**4**), and this also facilitated work on the five additional compounds. The optical properties of **4** were reassessed, and the negative rotation data obtained were invariant. The published configurations of each of the four amino acid residues were verified as shown in Figure 3. This involved acid-mediated hydrolysis of **4** (0.5 mg in 6 M HCL at 120 °C) followed by derivatization with Marfey's reagent (1-fluoro-2,4-dinitrophenyl-5-L-alanine amide, FDAA).³¹ The initial separation scheme, using a standard gradient of acetonitrile (CH₃CN) and water with 0.1% formic acid, did not provide sufficient separation between (2*S*,3*R*)-Thr and (2*S*,3*S*)-Thr or between (*S*)-Ser and (*R*)-Ser. These observations mirror those difficulties seen by others^{29,32} (Figures S25–S28, Supporting Information). Thus, gradient optimization steps were developed to achieve baseline resolution between these amino acid-FDAA diastereomers (Figures S25–S28, Supporting Information). A solvent system of 90:10 CH₃CN-MeOH as the organic solvent and 5% acetic acid in water as the aqueous solvent was found to provide accurate results.³² The Marfey's analysis confirmed the amino acid configurations previously published for kailuin D (**4**) as (2*S*,3*S*)-Ile, (*R*)-Leu (2), (2*S*,3*R*)-Thr, (*S*)-Ser, and (*R*)-Leu (1). Marfey's analysis was also completed on kailuin E (**5**), with the same absolute configuration deduced for **4** (Figures S25–28, Supporting Information).

Additional scrutiny of the NMR data previously reported for kailuin D (**4**), as noted above, revealed discrepancies in the lipid portion of the structure. This led to the conclusion that both the geometry of the double bond and the assignment of the allylic resonances were incorrect. Davidson et al.²⁶ reported an *E* geometry using a coupling-based argument and assigned the vinyl signals at δ_{H} 5.36 (δ_{C} 130.9) and δ_{H} 5.26 (δ_{C} 128.5) at positions 7 and 8 of the acyl chain, respectively. Closer examination revealed *Z* geometry by ¹³C NMR data and *J*-coupling values and also indicated a reversal of the assignments of 7 and 8 via 2D NMR experiments (Figures S2 and S3, Supporting Information). The acyl chain spin system and the position of the double bond were verified by HMBC and COSY experiments. These results confirmed that the diastereotopic proton resonances of position 2 (δ 2.47 and 2.54) correlated to a carbonyl resonance at δ 173.1, to which the amide of Leu-1 (δ 6.36) also correlated, thereby establishing the position of C-2 as adjacent to the N-terminal amide of Leu-1. The COSY correlations from position C-2 to C-9 showed C-6 (δ 2.02) is allylic to C-7 (δ 5.26), while C-9 (δ 1.97) is allylic to C-8 (δ 5.36). The ¹³C NMR resonances of these allylic positions (δ 26.6 and 27.2) are in agreement with ¹³C NMR shift analysis for the *Z* configuration, using benchmark data of δ_{C} 29 for *Z* and δ_{C} 35 for *E*.³⁰ Additionally, the resolution of the vinyl multiplets at 600 MHz in this work was a significant improvement over that reported at 500 MHz (Figure S2, Supporting Information), enabling the correct coupling constants to be extracted. Poor resolution in the vinyl multiplet region appears to have misled previous elucidation efforts. The vicinal coupling between C-7 and C-8 (*J* = 10.8 Hz) also supported the *Z* double-bond configuration, where *J* = 11 Hz is typical of *Z*, and *J* = 17 Hz is indicative of an *E* configuration.³⁰

To date, no attempts have been made to deduce the absolute configuration at the β -acyloxy position of the known kailuin analogues A–F (**1–6**). Also relevant is that more than 12 microbial-derived cyclic depsipeptides have been described possessing a β -acyloxy substructure (see Figure 1 and Figure S33, Supporting Information). An *R* configuration at

the β -acyloxy carbon has been deduced previously for six members of this collection including (a) solonamide A,¹⁹ unnarmicin A,²¹ and kahalide V³³ by Mosher's method; (b) tripropeptin C by chiroptical data of a β -hydroxy acid product;³⁴ and (c) peptidolipin B³⁴ and serratiomycin³⁶ by NMR NOE measurements, $^3J_{H-H}$ values, and ^{13}C NMR calculated δ s (Figure 4). However, similar to the situation with the kailuins, no assignments have been made for other members of this list including ngercheumicins D and E,²⁰ halobacillin,³⁷ and kahalalides Y and W (W was assigned only by biosynthetic analogy).³³ To date, no natural products of this type have been reported with an *S* configuration at the β -acyloxy carbon, although NMR properties for the peptidolipin B have been predicted via DFT calculations (see Figure 4).³⁵

Deducing the assignment of the β -acyloxy carbinol carbon for kailuins A–E (**1–5**) and new compounds kailuins G (**7**) and H (**8**), whose structures are all discussed below, was eventually accomplished, although it proved to be more challenging than initially expected. An obvious first step involved Mosher's analysis by preparing and examining *R/S*-MTPA (α -methoxy- α -trifluoromethylphenylacetic acid) esters of the β -hydroxyl group, and kailuin B (**2**) was chosen for this process. As noted above, this strategy has been successfully used by others, although such an analysis failed during the evaluation of the peptidolipins.³⁵ As described below, Mosher's method was tenuous for the kailuins and motivated the quest for back-up analysis. This was achieved by assembling a minidatabase of ^{13}C NMR chemical shift values. Shown below are that these ^{13}C δ data can provide a fast, general approach to assessing *R/S* configurations for almost any metabolite having a β -acyloxy moiety.

The Mosher's tactic began by ester cleavage on kailuin B (**2**) using lithium hydroxide. Two products, outlined in Scheme 2, were obtained and consisted of depsipeptide alcohol I (m/z 748.4856 [$M + Na$]⁺) (**9**) and a linear alcohol (m/z 758.8 [$M + Na$]⁺) (**10**). The major product **9** arose from intramolecular attack by the (*S*)-serine hydroxy group at the ester carbon. The hypothetical product **11**, potentially formed from attack by the (2*S*,3*R*)-Thr hydroxy group, was not observed. Alcohol I (**9**) was converted in an NMR tube to the bis esters *R*-MTPA (**12a**) and *S*-MTPA (**12b**) (Scheme 2)^{38,39} (both exhibited nominal m/z = 599 [$M + H + K$]²⁺ for molecular formula C₅₇H₈₁F₆N₅O₁₃). However, there were complications in measuring and interpreting the δ_{S-R} patterns. Anomalous 1H δ values can arise for protons in proximity to multiple MTPA residues,⁴⁰ and this is apparent in the strange data pattern shown in Figure 4 (panel A) at Ser: NH δ_{S-R} = +0.076, H α δ_{S-R} = -0.036, H β δ_{S-R} = +0.018, +0.111). Unfortunately, no useful δ data were observed for the nine-carbon side chain flanking the CO-MPTA group because the resonances of **12a/12b** appeared as unresolved multiplets. This same situation also confounded the Mosher approach to the peptidolipins, possessing a 23-carbon side chain,³⁵ but it was not a problem for the three five-carbon side chain containing compounds^{19,21,33} (Figure S32, Supporting Information). The only remaining useful data were minimal and consisted of δ_{S-R} = -0.059 at C-2, suggesting an *R* β -acyloxy configuration. Correspondingly, this was identical in sign and magnitude to data reported at this same position (see Figure S32, Supporting Information) for the *R* β -acyloxy of solo-namide A (δ_{S-R} = -0.04),¹⁹ solonamide B (δ_{S-R} = -0.04),¹⁹ unnarmicin A (δ_{S-R} = -0.02),²¹ and kahalide V (δ_{S-R} = -0.16/-0.18).³³

Finally, the $\delta_{S-R} = +0.030$ at Thr supported the 3R configuration at this amino acid group, in agreement with the assignment obtained (discussed above) from Marfey's analysis.

The power and speed in using ^{13}C NMR δ trends for configuration analysis is well accepted; however to do so requires a set of diagnostic data.³⁰ There is relevant information in the literature for carbons associated with a β -acyloxy functionality, but these data have not yet been compiled or analyzed. The collection in Figure 4 panel B provides values for β -acyloxy ^{13}C NMR chemical shifts of 14 compounds at the key α , β , and γ positions. Unfortunately, the chemical shift trends for the α position are not useful, whereas the data from the other two positions provide a pattern for assigning the configuration at $C\beta$ as *R* or *S*. Important benchmark information is contained in the first three entries, which present experimental *R*-peptiolipin B ^{13}C shifts ($\delta_{C\beta}$ 72.6, $\delta_{C\gamma}$ 32.5)³⁵ alongside those from DFT calculations for *R*-peptiolipin B ($\delta_{C\beta}$ 74.1, $\delta_{C\gamma}$ 35.7) and *S*-peptiolipin B ($\delta_{C\beta}$ 77.5, $\delta_{C\gamma}$ 40.6).³⁵ Other diagnostic insights can be derived from the data available for an additional five compounds definitively assigned with an *R*- β -acyloxy configuration (solonamide A,¹⁹ unnarmicin A,²¹ serratiomycin,³⁶ triopeptin,³⁴ and kahalalide V³³), whose shift values are $\delta_{C\beta}$ 71–73 and $\delta_{C\gamma}$ 34–36. Thus, our proposed analysis framework consists of (a) assigning an *R* configuration when $\delta_{C\beta} \sim 74/\delta_{C\gamma} \sim 36$ and (b) assigning an *S* configuration when $\delta_{C\beta} \sim 77/\delta_{C\gamma} \sim 40$.

The patterns shown in Figure 4 panel B, interpreted using the rules for *R/S* configuration assignment at the β -acyloxy summarized above, were applied to reexamine the kailuins. Using the experimental data collected (Tables S2 and S4, Supporting Information) allows an *R* configuration to be assigned for kailuin B (**2**) ($\delta_{C\beta}$ 73.2, $\delta_{C\gamma}$ 35.5), kailuin C (**3**) ($\delta_{C\beta}$ 73.2, $\delta_{C\gamma}$ 35.6), kailuin D (**4**) ($\delta_{C\beta}$ 73.1, $\delta_{C\gamma}$ 35.1), and kailuin E (**5**) ($\delta_{C\beta}$ 73.0, $\delta_{C\gamma}$ 35.4), as well as for the new compounds described below: kailuin G (**7**) ($\delta_{C\beta}$ 73.2, $\delta_{C\gamma}$ 35.6) and kailuin H (**8**) ($\delta_{C\beta}$ 73.2, $\delta_{C\gamma}$ 35.6). Extending this analysis allows an *R* configuration to also be assigned, based on literature data ($\delta_{C\beta}$ 73.0, $\delta_{C\gamma}$ 35.3),²⁴ for kailuin A (**1**). Employing this same logic allows four other compounds to now be assigned as *R* including kahalalides W and Y,³³ halobacillin,³⁷ and ngercheumicin D²⁰ (Figure 4).

In addition to kailuin D (**4**), the other five pure compounds (**2**, **3**, **5**, **7**, and **8**) obtained from the HPLC fractions shown in Scheme 1 all had negative optical rotations. They could be best tracked using the ESIMS m/z $[\text{M} + \text{H}]^+$ values consisting of 726, 740, and 754. Structures for kailuins B, C, and E (**2**, **3**, and **5**) were dereplicated by comparing HAMS and NMR data to literature values.^{26–28} Fraction H6 contained a compound with an m/z of 740 $[\text{M} + \text{H}]^+$ and a molecular formula calculated from HAMS data as $\text{C}_{38}\text{H}_{69}\text{N}_5\text{O}_9$. This molecular formula was unique compared to previously isolated kailuins and represented the loss of a methyl group from kailuin E (**5**). The ^1H and ^{13}C NMR data (shown in Table 1) indicated that its tetrapeptide core remained unchanged compared to the other known kailuins. When combined with the 2D NMR data, the only difference in this compound was the length of the alkyl chain. Taken together, these data represent a new member of the kailuin class of compounds, and it was given the name kailuin G (**7**). Fraction H9 contained a compound with an m/z of 754 $[\text{M} + \text{H}]^+$. HAMS confirmed a molecular formula of $\text{C}_{39}\text{H}_{69}\text{N}_5\text{O}_9$, which was the same as kailuin E (**5**). The ^1H and ^{13}C NMR data again confirmed that its tetrapeptide core remained unchanged. The ^1H – ^{13}C HMBC and ^1H – ^1H

COSY analysis confirmed the presence of a terminal isopropyl group on the alkyl chain. This suggested the occurrence of a new kailuin analogue, which has been named kailuin H (**8**). Biosynthetically, the same gene cluster likely produces each of the kailuin compounds isolated, so it is reasonable to assume that all of the isolated kailuins have the same configuration at each of the amino acid subunits as well as at the C-3 position. Therefore, these compounds were assigned the same absolute configuration as the previously isolated kailuins. Finally, all of the kailuins isolated here exhibited negative $[\alpha]_D$ values.

Although the kailuins have shown antimicrobial activity^{27,28} and low micromolar cytotoxicity against several tumor cell lines,²⁶ no mechanism of action has been reported for these activities. To assess the biological activity of the kailuins, the small library of compounds on hand was screened against the tumor cell lines described in previous publications to provide insights into their structure–activity relationships and further explore their mechanistic target(s).²⁶ The role of the depsipeptide core contribution to the cytotoxicity represented an additional, important issue, because this could lead to next-generation simplified bioactive analogues. To explore these ideas, we employed a standard synthetic methodology to prepare two reduced complexity compounds for screening. The strategies outlined in Scheme 3 utilized fluoroenylmethoxy-carbonyl (Fmoc) solid-phase chiral peptide synthesis followed by solution-phase cyclization and provided two compounds, which both showed negative optical rotation, including the kailuin core (**13**) ($[\alpha]_D^{24} = -45.8$) and the kailuin lactam (**14**) ($[\alpha]_D^{24} = -1.6$).

The detailed synthetic strategy employed in the synthesis of the kailuin core (**13**) is shown in Scheme 3. It was centered on microwave-assisted couplings and deprotections,⁴¹ along with an expedient solution-phase cyclization protocol. The linear peptide was synthesized on 2-chlorotrityl polystyrene resin using the Fmoc protection group tactic. Microwave couplings were carried out using HBTU (*N,N,N',N'*-tetramethyl-*O*-(1*H*-benzotriazol-1-yl)uronium hexafluorophosphate) and 1-hydroxy-7-azabenzotriazole (HOAt) (10 min, 50 °C, 12 W), while deprotections were carried out with 2% DBU (1,8-diazabicyclo[5.4.0]undec-7-ene) and 2% piperidine in DMF (5 min, 50 °C). Synthesis of the protected 3-hydroxypropionic acid monomer was accomplished via monoprotection of 1,3-propanediol⁴² followed by oxidation of the alcohol directly to the carboxylic acid with Confer's reagent that was generated in situ.⁴³ Coupling of this monomer was achieved using *N,N'*-diisopropylcarbodiimide (DIC) (DMF, 1 h, twice). Removal of the TBDPS (*tert*-butyldiphenylsilyl) group was accomplished using TBAF (tetra-*n*-butylammonium fluoride) in THF overnight. The last amino acid, Fmoc-(2*S*,3*S*)-Ile, was coupled onto the unprotected alcohol using 5 equiv of Fmoc-(2*S*,3*S*)-Ile, 5 equiv of DIC, 0.25 equiv of DMAP (4-dimethylaminopyridine), and 1 equiv of DIPEA (*N,N*-diisopropylethylamine) in DMF for 45 min twice.⁴⁴ In order to prevent nucleophilic displacement of the ester bond by piperidine, the Fmoc group of this amino acid was instead removed using the non-nucleophilic base DBU (5% v/v in DMF, RT, 5 min).

The deprotected linear peptide was cleaved off resin, and residual TFA was removed in vacuo overnight to prevent activation of the acid and subsequent N-terminal capping. It was found that a mixture of THF and CH₃CN (1:1 v/v) under high dilution (1 mg crude peptide/mL solvent) provided a cyclization solvent system that was easily removed via

rotary evaporation. The coupling reagent COMU ((1-cyano-2-ethoxy-2-oxoethylideneaminoxy)dimethylamino-morpholino-carbenium hexafluorophosphate) was used as the cyclization reagent, which afforded complete cyclization of the peptide within 20 min. This represented a tremendous improvement over the commonly reported reaction times of 16 h.⁴⁵ It has been reported previously that COMU may not provide an efficient cyclization reagent,⁴⁶ but in this system, however, it enabled expedient macrolactamization. Moreover, global side chain deprotection using 50% TFA in CH₂Cl₂ in the presence of COMU leads to many undesired side reactions (unpublished data). This problem was avoided by removing the COMU byproducts via flash chromatography with high recovery prior to deprotection. Final reversed-phase HPLC purification yielded the kailuin core (**13**) in 40% yield, based on resin loading, over 14 steps. An overview of this sequence is shown in Scheme S1, Supporting Information.

The kailuin lactam (**14**), devoid of the lipid chain, was envisioned as a key compound to test side-by-side with the lactone for their potential to modulate the bioactivity. The lactam was concisely prepared by a multistep chiral synthesis sequence (Scheme S2, Supporting Information), using a peptide synthesizer with room-temperature couplings without HOAt. The same 20 min CH₃CN/THF COMU cyclization conditions were utilized, and this peptide was obtained in 26.4% overall yield.

The mini-library consisting of compounds **2–5**, **7**, **8**, **13**, and **14** was screened against a human colon tumor (HCT-116) cell line to investigate their cytotoxicity and preliminary structure-activity relationships.⁴⁷ The kailuins (**2–5**, **7**, **8**) displayed weak activity in the assay used against HCT-116, a human colon cancer cell line, with IC₅₀ values of 17–32 μ M, as shown in Table 2. Previous publications have reported activity against human lung (A-549), breast (MCF-7), and colon (HT-29) tumor cell lines in the 3–6 μ M range,²⁶ representing an order of magnitude difference compared to results found in this work. To determine if the observed differences were due to selectivity against certain cell lines, kailuin D (**4**) was run against the MCF-7 breast cancer cell line reportedly used in previous studies. The IC₅₀ in our assay was 39 μ M and did not compare to the 4 μ M IC₅₀ in the previous report.²⁶ The synthetic kailuin depsipeptide core (**13**) and lactam (**14**) were inactive against HCT-116 cells at >100 μ M IC₅₀ values, and Table 2 summarizes these overall differences in assay results.

Due to the disparities between the current and published IC₅₀ values described above for kailuins D and E (**4**, **5**), they were submitted for additional screening. First, the compounds were examined by cytological profiling (CP).⁴⁸ This screening tool uses automated microscopy and image analysis to gain insights into phenotypic features. The CP assay develops “fingerprints” obtained by comparing the cytotoxic phenotypic effects on HeLa cells to a library of 500 reference compounds with known biological mechanisms of action. Similar to the initial screens against solid tumor cell lines, **4** and **5** showed only weak cytotoxicity in the CP assay. The phenotypic “fingerprint” of this weak cytotoxicity did not cluster to any compounds with known mechanisms of cancer cell cytotoxicity. In addition, compounds **4** and **5** were submitted for screening in the BioMAP assay.⁴⁹ This assay tests compounds against 15 bacterial strains and compares the phenotypic response to 72

antibiotics with known mechanisms of action. The BioMAP assessment showed only weak effects with no clustering to any antibiotics in the compound library.

In summary, six kailuins (**2–5**, **7**, and **8**), a rare class of cyclic depsipeptides, were isolated and characterized from a marine-derived Gram-negative bacterium, *P. halotolerans*. New insights have been obtained on the kailuins and two synthetic derivatives, and several outcomes contained in previous publications have been re-examined and clarified. Two new analogues have been isolated (**7** and **8**), and the double-bond geometry of **4** has been revised. The basis for absolute configuration assignments in each of the constituent depsipeptide subunits was re-examined. An NMR ^{13}C shift database was created and used to determine the previously unassigned configuration as *R* at the β -acyloxy position of all but one of the previously isolated kailuins. This strategy was also extended in the *R/S* configuration analysis of other β -acyloxy-containing natural products. Additionally, it appears that the bioactivity properties of the kailuins have been overstated in the past. The screening responses measured here, including the cytotoxic data of Table 2, cytological profiling, and BioMAP antimicrobial evaluations (data not shown), revealed weak to no activity. The biological activity properties reported in previous publications were not reproduced. Such an outcome is surprising because other members of this class have been reported to exhibit activity, including bacteriostatic,³⁶ quorum-sensing interference,²² antifungal effects,⁵⁰ and mild cytotoxicity to HCT-116 cells.⁴⁰

Moving forward, it would appear that the provisional taxonomic identification of *Vibrio* sp. described in each of the previous reports on the kailuins should be revisited and possibly revised to *Photobacterium*. The discrepancy in taxonomic identification of these organisms is most likely due to the publication date of initial work on the kailuins (in 1997 and 2000), which preceded the description (2006) of the type strain, *P. halotolerans* sp. nov.²⁴ There are some important next steps to be suggested. Further study and bioactivity assessment are warranted for metabolites from the 25 unstudied *Photobacterium* species. Strains of note include the fully sequenced *P. leiognathi* subsp. *mandapamensis*⁵¹ and *P. gangwense*, which was originally isolated from seawater.⁵² Little is known about the secondary metabolism of these organisms, and minimal work has been done to discover quorum-sensing compounds potentially produced by these organisms. For example, preliminary secondary metabolite gene cluster analysis of *P. leiognathi* subsp. *mandapamensis* by antiSMASH⁵³ did not reveal any clusters that appear to produce typical quorum-sensing compounds (unpublished data). Currently, our culture collection contains 10 different *Photobacterium* strains, and studies on each are currently under way.

Experimental Section

General Experimental Procedures

Optical rotations were performed on a JASCO P-2000 polarimeter. All NMR experiments were run on a Varian Unity spectrometer (500 and 125 MHz for ^1H and ^{13}C , respectively) or Varian INOVA spectrometer (600 and 150 MHz for ^1H and ^{13}C , respectively) equipped with a cryoprobe. High-accuracy mass spectrometry measurements were recorded for all compounds (except **14**) using an Applied Biosystems Mariner electrospray ionization time-of-flight (ESITOF) mass spectrometer. HAMS measurements for **14** were obtained using a

Thermo Velos Pro electrospray ionization hybrid ion trap–orbitrap mass spectrometer. Prefractionation HPLC was performed using a Phenomenex Gemini-NX C₁₈ (50 × 21.1 mm, 5 μm) column. Semipreparative HPLC fractions were generated using a Phenomenex Luna 5 μm C₁₈ (250 × 10 mm, 5 μm) column. Analytical LC-MS analysis was performed on samples at a concentration of approximately 15–20 mg/mL, using a reversed-phase 150 × 4.60 mm 5 μm C₁₈ Phenomenex Luna column in conjunction with a 4.0 × 3.0 mm C₁₈ (octadecyl) guard column and cartridge (holder part number: KJ0-4282; cartridge part number: AJ0-4287, Phenomenex, Inc., Torrance, CA, USA). An injection volume of 15 μL and a solvent flow rate of 1 mL/min were used. Injections were monitored using a Waters model 996 photodiode array UV detector. The elution was subsequently split (1:1) between a SEDERE model 55 evaporative light scattering detector (ELSD) and an Applied Biosystems Mariner electrospray ionization time-of-flight mass spectrometer. Peptides were purified using an HPLC equipped with an XBridge BEH130 5 μm 19 × 150 C₁₈ column. Synthetic preparation of intermediates, kailuin core (**13**) and kailuin lactam (**14**), involved the purchase of 2-chlorotriptyl chloride resin from Aapptec. Fmoc-protected amino acids were purchased from Aapptec, Novabiochem, or P3 Biosystems. HOAt was also purchased from Aapptec. HBTU and TBDPSCI were purchased from Oakwood Chemical. TFA and CH₂Cl₂ were purchased from Fisher. DMF, EtOAc, and hexanes were purchased from Macron, and 1,3-propanediol was purchased from Acros. All reagents were used without further purification.

Biological Material and Taxonomic Identification

Strain M128SB283Ax was isolated from intertidal sediment from Manresa State Beach, Watsonville, CA. After drying in air, a small amount of the sediment was placed on *E. coli*-streaked AWCX agar plates¹² made with SWS⁵⁴ and 25 mg of cycloheximide. A nearly transparent swarming bacterium was transferred to VY2 agar plates³⁹ with SWS and Zobell Marine Broth (DIFCO) plates until a pure culture was obtained. Genomic DNA from strain M128SB283Ax was isolated from the cell mass that was scraped from CY-SWS agar plates¹² using the Wizard Genomic DNA purification kit (Promega). The eubacterial primers 27F (5' AGA GTT TGA TCC TGG CTC AG 3') and 1492R (5' ACG GCT ACC TTG TTA CGA CTT 3') were used to amplify 16S rRNA by PCR using QIAGEN 2X master mix, with 25 pmol of each primer, and yielded approximately 300 ng of genomic DNA. PCR was performed with an Eppendorf Mastercycler personal thermocycler under the following conditions: denaturation at 94 °C for 2 min, followed by 25 cycles of denaturation at 94 °C for 1 min, annealing at 51 °C for 1 min, extension at 72 °C for 1.5 min, terminated by a final extension at 72 °C for 7 min. PCR cleanup and sequencing was performed by the University of California Berkeley Sequencing Facility. Forward and reverse reads were analyzed using FinchTV and assembled into a 1379 bp fragment of 16S rRNA. Initial analysis via the BLAST server of the National Center for Biotechnology Information (NCBI) revealed a match to the *Photobacterium* genus.⁵⁵ The sequence was aligned against all *Photobacterium* species in the NCBI's nonredundant nucleotide database (RefSeq) using MAFFT (G-INS-i strategy with 1PAM/K=2).⁵⁶ A phylogenetic tree was built using the neighbor-joining method (total of 5000 bootstraps) on the conserved regions of the alignment, indicating that strain M128SB284Ax is a variant of *P. halotolerans*.⁵⁷ The DNA

sequence was deposited in GenBank with accession number KJ755052. Cultures are maintained as a cryopreserved glycerol stock at University of California, Santa Cruz.

Culture Conditions

A starter culture of bacterium strain M128SB283Ax was prepared in MD1 medium¹² in 75% seawater⁵⁴ and rotary shaken at 200 rpm at 30 °C for 7 days. For scale-up preparation, eight 4 L baffled Delong flasks, each containing 2 L of sterile MD1 medium in 75% seawater with 2% w/v XAD-7 adsorbent resin, were inoculated with 10 mL of starter culture. The flasks were shaken at 200 rpm at 30 °C for 20 days.

Biological Assays

Data from the cytological profiling screen involved an analysis of the cytotoxic phenotypic effects observed for kailuins D (**4**) and E (**5**) and the kailuin core (**13**) and kailuin lactam (**14**) against HeLa cells. The profiles of **4**, **5**, **13**, and **14** were compared against a panel of 500 biologically active molecular structures with diagnostic cytotoxic phenotypic effects against HeLa cells, as is described in detail elsewhere.⁴⁸ The IC₅₀ values reported against HCT-116 cell lines were obtained using methods described previously.⁴⁷

Extraction and Isolation

Resin and cell mass were vacuum-filtered from the fermentation broth and exhaustively extracted with methanol, then acetone. The crude extract was evaporated to dryness and then partitioned between water and dichloromethane to yield 450 mg of organic extract. Half of the organic extract was prefractionated via HPLC using CH₃CN–H₂O, 10 mL/min flow rate, and the following step gradient: 0% CH₃CN for 0.5 min, linear gradient to 40% CH₃CN for 0.6 min, hold at 40% CH₃CN for 0.4 min, linear gradient to 70% CH₃CN over 1 min, hold at 70% CH₃CN for 0.4 min, linear gradient to 100% CH₃CN over 0.5 min, hold at 100% CH₃CN for 10 min. Prefraction collection times were as follows: F0: 0.0–2.0 min, F1: 2.0–3.5 min, F2: 3.5–5.0 min, F3: 5.0–6.5 min, F4: 6.5–8 min, F5: 8–9.5 min, F6: 9.5–14.0 min (see Scheme 1). Prefractions 3–5 (47 mg) were combined and subjected to semipreparative HPLC using 80% CH₃CN–20% H₂O (with 0.1% formic acid) at 4 mL/min, UV absorbance detection at 210 nm, to yield 0.8 mg of **3** (*t*_R = 13.5 min), 2.0 mg of **2** (*t*_R = 14.4 min), 3.2 mg of **4** (*t*_R = 17.6 min), 1.7 mg of **7** (*t*_R = 19.4 min), 1.7 mg of **8** (*t*_R = 24.8 min), and 4.0 mg of **5** (*t*_R = 26.9 min).

Kailuin B (2)—white film; [*α*]_D²⁴ –20.1 (*c* 0.9, MeOH); HAESITOFMS *m/z* [M + K]⁺ 764.4591 (calcd for C₃₇H₆₇N₅O₉K, 764.4570); for ¹H and ¹³C NMR data, see Table S2, Supporting Information.

Kailuin C (3)—white film; [*α*]_D²⁴ –14.5 (*c* 0.55, MeOH); HAESITOFMS *m/z* [M + K]⁺ 764.4573 (calcd for C₃₇H₆₇N₅O₉K, 764.4570); for ¹H and ¹³C NMR data, see Table S3, Supporting Information.

Kailuin D (4)—white film; [*α*]_D²⁴ –15.0 (*c* 0.8, MeOH); HAESITOFMS *m/z* [M + K]⁺ 790.4739 (calcd for C₃₉H₆₉N₅O₉K, 790.4727); for ¹H, ¹³C, and 2D NMR data, see Figures S4–S8 and Table S2, Supporting Information.

Kailuin E (5)—white powder; $[\alpha]_D^{24} -19.4$ (*c* 0.1, MeOH); HAESITOFMS m/z 776.5134 (calcd for $C_{39}H_{71}N_5O_9Na$, 776.5144 $[M + Na]^+$); for 1H , ^{13}C , and 2D NMR data, see Table S3, Supporting Information.

Kailuin G (7)—white film; $[\alpha]_D^{24} -20.0$ (*c* 0.45, MeOH); HAESITOFMS m/z $[M + Na]^+$ 762.4963 (calcd for $C_{38}H_{69}N_5O_9Na$, 762.4988); for 1H , ^{13}C , and 2D NMR data, see Figures S9–S11 and Table S2, Supporting Information.

Kailuin H (8)—white film; $[\alpha]_D^{24} -21.7$ (*c* 0.6, MeOH); HAESITOFMS m/z $[M + K]^+$ 792.4875 (calcd for $C_{39}H_{71}N_5O_9K$, 792.4883); for 1H , ^{13}C , and 2D NMR data, see Figures S12–S14 and Table S2, Supporting Information.

Marfey's Analysis of Kailuin D (4) and Kailuin E (5)

Marfey's analysis³¹ was performed to determine the absolute configuration of each amino acid contained in **4** and **5** (Figures S25 and S26, Supporting Information). Briefly, 0.5 mg of each compound was dissolved in 6 M HCl and heated at 100 °C for approximately 18 h. After heating, the sample was dried under reduced pressure, redissolved in 50 μ L of water, and transferred to a 1.5 mL centrifuge tube. Aliquots consisting of 50 μ L of 50 mM of each enantiomer of each standard amino acid were treated independently in 1.5 mL centrifuge tubes. To each standard and sample were added 100 μ L of 1% FDAA and 20 μ L of 1 M $NaHCO_3$. Tubes were capped and heated in a 40 °C water bath with periodic mixing for 1 h. After cooling to room temperature, 10 μ L of 2 M HCl was added to each tube. The mixtures were dried under reduced pressure and redissolved in 200 μ L of 9:1 MeOH–H₂O. Samples were diluted further to one-tenth of their original concentration with 9:1 MeOH–H₂O prior to LC-MS analysis. The configuration of the Leu and Ile amino acids was confirmed using a standard HPLC gradient using CH₃CN and water spiked with 0.1% formic acid as the mobile phase. To achieve separation of the FDAA derivatives of (*R*)- and (*S*)-Ser and (2*S*, 3*R*)- and (2*S*, 3*S*)-Thr, a mixture of 90:10 CH₃CN–MeOH was used as the organic solvent and 5% acetic acid in water was used as the aqueous solvent. Details of the gradient profiles, columns, flow rates, and chromatographic method development are described elsewhere (Figures S25–S28, Supporting Information).

Synthesis and Purification of Kailuin B Depsipeptide Alcohol 1 (9)

A 2.9 mg (3.99 μ mol) sample of kailuin B (**2**) was dissolved in 2175 μ L of MeOH in a 20 mL scintillation tube. Then, 725 μ L of a 0.025 M LiOH solution was added to the dissolved depsipeptide to make a 1 mg/mL reaction solution. The solution was briefly sonicated and placed in a 30 °C incubator overnight. The reaction was then quenched with equimolar (0.025 M) HCl and dried on a SpeedVac. The dried residue was washed with anhydrous THF three times to solubilize the product and the resulting LiCl salt, to yield 1.2 mg of a mixture of **9** (m/z 725) and **10** (m/z 758). Separation with a CH₃CN–H₂O gradient from 50% to 100% acetonitrile over 20 min (1 mL/min) using a Kinetex C₁₈ column (2.6 μ m, 100 \times 4.6 mm, Phenomenex) yielded 0.6 mg of **9** and 0.2 mg of **10**.

Kailuin B depsipeptide alcohol I (9)—white solid; HAESIMS m/z 748.48310 $[M + Na]^+$ (calcd for $C_{37}H_{67}N_5O_9Na$, 748.48562). See Figure S29–S31 (Supporting Information) for relevant 1H and 2D NMR data.

Kailuin B linear alcohol (10)—white solid; nominal m/z 758.8 $[M + Na]^+$.

Preparation of the (*R*)- and (*S*)-MTPA Ester Derivatives

Compound **9** (0.6 mg) was dried in a vacuum desiccator overnight. The dried residue was dissolved in deuterated pyridine (666 μL), and equal volumes (333 μL) were transferred into two 5 mm $CHCl_3$ Shigemi NMR tubes under a N_2 gas stream. (*S*)-(+)- α -Methoxy- α -(trifluoromethyl)phenylacetyl ((*S*)-MTPA) chloride (2 μL) was added into the NMR tube and lightly shaken to mix **9** evenly with the reagent. In a separate NMR tube, (*R*)-(–)- α -methoxy- α -(trifluoromethyl)phenylacetyl chloride ((*R*)-MTPA) (2 μL) was added and shaken to mix **9** with the reagent. After 4 h the reaction mixture showed a nominal mass spectrometric signal (m/z 599.49) representing Mosher esterification to C-3 and the (2*S*,3*R*)-Thr *C* β hydroxy group. Relevant 1H NMR data used for Mosher's analysis are described below (see also Figure S32, Supporting Information)

(*R*)-MTPA ester (12a)—white solid; 1H NMR of **12** (600 MHz, pyridine- d_5) δ 9.69 (1H, d, J = 6.96 Hz, Ser NH), 5.28 (1H, m, Ser H α), 4.55 (1H, dd, J = 10.68, 5.4 Hz, Ser H β , Hb), 4.33 (1H, dd, J = 10.98, 5.7 Hz, Ser H β , Hb), 2.19 (2H, m, H-2), 1.47 (3H, d, J = 6.06, Thr H γ).

(*S*)-MTPA ester (12b)—white solid; 1H NMR of **12** (600 MHz, pyridine- d_5) δ 9.76 (1H, d, J = 5.58 Hz, Ser NH), 5.25 (1H, m, Ser H α), 4.56 (1H, dd, J = 10.68, 5.4 Hz, Ser H β , Hb), 4.35 (1H, dd, J = 10.68, 5.3 Hz, Ser H β , Hb), 2.13 (2H, m, H-2), 1.50 (3H, d, J = 6.18, Thr H γ).

Peptide Purification

Peptides were purified after solution-phase cyclization on a Biotage Isolera Prime system equipped with a KP-C18-HS 12 g column eluting with H_2O – CH_3CN modified with 0.1% TFA. Peptides were purified after global deprotection on a Waters mass-directed preparative HPLC system eluting with H_2O – CH_3CN modified with 0.1% formic acid.

Loading Fmoc-S-Leucine-OH onto 2-Chlorotrityl Chloride Resin

A 3.0 g aliquot of Fmoc-S-Leu-OH was dried under a vacuum for 24 h. A 5 g bottle of 2-chlorotrityl chloride resin (200–400 mesh; 1% DVB) was stored in a desiccator under vacuum prior to use. Anhydrous CH_2Cl_2 was added to the Fmoc-S-Leu-OH, followed by dry DIPEA (4 equiv, 5.6 mL). The solution was transferred by syringe to a flame-dried round-bottom flask containing 5.0 g of resin and a stir bar. The resin and solution were stirred gently at room temperature for 3 h. After 3 h, the resin and solution were transferred to a polypropylene synthesis vial containing a fritted disk and fitted with a Teflon stopcock. The resin was drained and rinsed with CH_2Cl_2 (3×30 mL), DMF (3×30 mL), and again with CH_2Cl_2 (3×30 mL). The remaining resin was treated with a solution of CH_2Cl_2 , methanol, and DIPEA (17:2:1 respectively, 2×30 min), in order to cap any unreacted linker. The resin

was dried thoroughly, and a 10 mg aliquot was taken for use in determining the loading value.

Determination of Resin Loading by the Fmoc Cleavage Method

A sample of dry resin (10 mg) was transferred to a microcentrifuge tube and allowed to swell in 800 μL of DMF. After 15 min, 200 μL of piperidine was added. The resin and solution were vortexed to effect good mixing and allowed to sit for an additional 15 min. After the Fmoc cleavage was complete, 10 μL of the solution was transferred to a quartz cuvette and diluted with 990 μL of DMF. The absorbance was measured at $\lambda = 301 \text{ nm}$. Using an extinction coefficient of $7800 \text{ Lmol}^{-1} \cdot \text{cm}^{-1}$, the loading value was determined to be 1.6 mmol of Fmoc-S-Leu-OH per gram of resin.

Preparation of 3-[(*tert*-Butyldiphenylsilyl)oxy]propan-1-ol

To a round-bottom flask charged with CH_2Cl_2 (10 mL) were added 1,3-propanediol (0.54 mL, 7.5 mmol) and DIPEA (1.96 mL, 11.25 mmol). TBDPSCl (2.04 mL, 7.88 mmol) was slowly added dropwise, and the reaction was allowed to proceed under N_2 for 15 h at room temperature. The reaction was reduced in vacuo, redissolved in ethyl acetate (100 mL), and washed with saturated citric acid ($3 \times 50 \text{ mL}$), followed by 0.5 M HCl (50 mL). The combined aqueous layers were back-extracted with ethyl acetate (50 mL). The combined organic layers were washed with brine (50 mL) and dried over sodium sulfate. The product was purified via flash chromatography (3% EtOAc–hexanes to 30% EtOAc–hexanes) and concentrated to yield the title compound (1.69 g, 70% yield) as a translucent, colorless solid. The observed TLC $R_f = 0.5$ 30% EtOAc–hexanes, silica gel. ^1H NMR (500 MHz, CDCl_3) δ 1.06 (16H, s), 1.82 (3H, p $J = 5.6 \text{ Hz}$), 2.06 (1H, br s), 3.85 (6H, td, $J = 5.6, 2.6 \text{ Hz}$), 7.37–7.48 (6H, m), 7.68 (4H, dd, $J = 8.0, 1.6 \text{ Hz}$); ^{13}C NMR (125 MHz, CDCl_3) δ 19.3, 27.1, 34.4, 62.1, 63.4, 127.9, 130.0, 133.4, 135.7; LC-ESIMS m/z 278 (8), 237 (M – Ph+) (12), 199 (30), 158 (96), 119 (8), 118 (29), 117 (100), 83 (13).

Preparation of 3-[(*tert*-Butyldiphenylsilyl)oxy]propanoic Acid

A 1.6 g (5.1 mmol) amount of 3-[(*tert*-butyldiphenylsilyl)oxy] was dissolved in 15 mL of DMF and added to a round-bottom flask. To this was added pyridinium HCl (4.13 g, 35.7 mmol) followed by a slow addition of $\text{K}_2\text{Cr}_2\text{O}_7$ (5.25 g, 17.6 mmol), and the reaction was allowed to stir overnight. The reaction was cooled to 4°C , and 3 g of Celite was added, followed by 40 mL of H_2O and 20 mL of diethyl ether. This mixture was stirred at 4°C for 45 min, then filtered over Celite. The aqueous layer was extracted with diethyl ether ($3 \times 30 \text{ mL}$). The combined organic layers were washed with 1 M HCl (50 mL) and saturated brine (50 mL), then dried over sodium sulfate. The product was purified via flash chromatography (3% EtOAc– CH_2Cl_2 to 30% EtOAc– CH_2Cl_2) and concentrated to yield the target compound (0.4 g, 24% yield) as a white solid. The observed TLC $R_f = 0.43$ 30% EtOAc–Hex 1% acetic acid, silica. ^1H NMR (500 MHz, chloroform- d) δ 1.04 (s, 9H), 2.61 (t, $J = 6.2 \text{ Hz}$, 2H), 3.95 (t, $J = 6.2 \text{ Hz}$, 2H), 7.35–7.48 (m, 6H), 7.67 (dd, $J = 7.6, 1.4 \text{ Hz}$, 4H); ^{13}C NMR (125 MHz, CDCl_3) δ 19.3, 26.9, 37.7, 59.7, 127.9, 129.9, 133.5, 135.7, 178.0; LCESIMS m/z (relative intensity) 351 (M + Na) (6), 292 (17), 251 (M – Ph^+) (100), 172.7 (7), 118 (14), 83 (17).

Kailuin core (13)—white powder; $[\alpha]^{24}_{\text{D}} -45.8$ (c 1.55, MeOH); HAESITOFMS m/z 600.3603 $[\text{M} + \text{H}]^+$ (calcd for $\text{C}_{28}\text{H}_{50}\text{N}_5\text{O}_9$, 600.3602 $[\text{M} + \text{H}]^+$); for ^1H and ^{13}C NMR data, see Figures S16–S19 and Table S5, Supporting Information.

Kailuin lactam (14)—white powder; $[\alpha]^{24}_{\text{D}} -1.6$ (c 1.25, MeOH); HAESITOFMS m/z 599.37705 $[\text{M} + \text{H}]^+$ (calcd for $\text{C}_{28}\text{H}_{51}\text{N}_6\text{O}_8$, 599.37684 $[\text{M} + \text{H}]^+$); for ^1H and ^{13}C NMR data, see Figures S20–S24 and Table S5, Supporting Information.

Supplementary Material

Refer to Web version on PubMed Central for supplementary material.

Acknowledgments

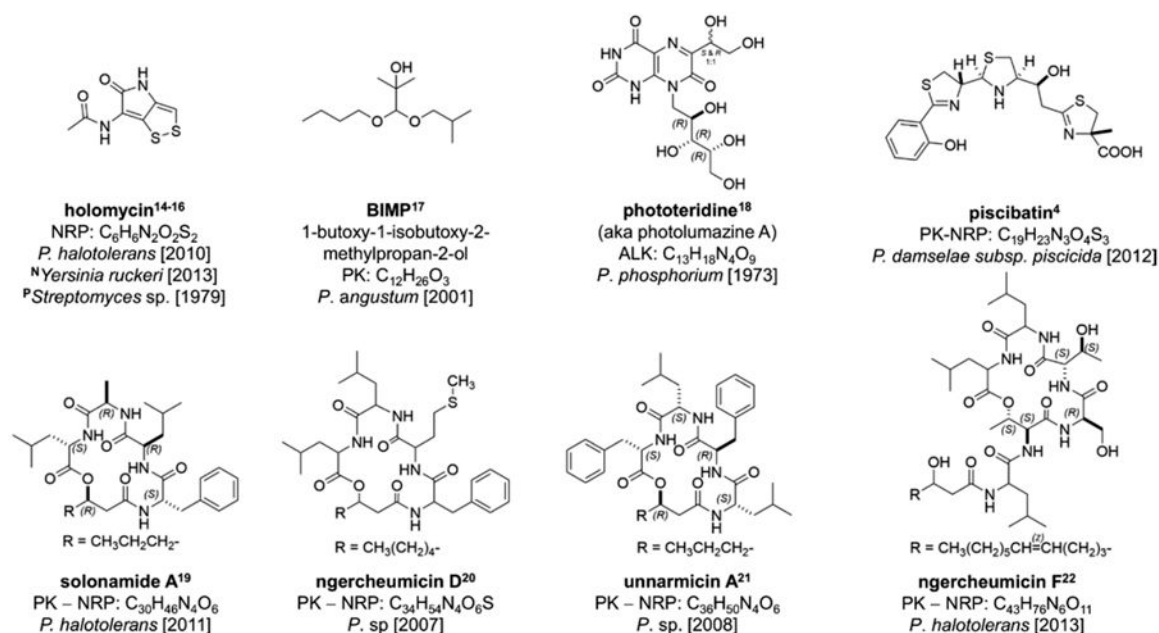
This work was supported by grants from the NSF (CHE 1214065) (P.C.) and NIH (R01 CA 47135) (P.C.). We also acknowledge additional funding from NIH (R01GM084530) (R.S.L.) and an NSF award (CHE 1427922) for MS instrumentation. The authors would like to acknowledge W. Bray at the UCSC Chemical Screening Center for assistance with cytological profiling and K. Tenney for collection of the sediment sample. Also, P. Dunlap at the University of Michigan is acknowledged for sample exchanges, guidance, and confirmation of bacterial taxonomy. The authors also wish to acknowledge S. Loveridge and H. Lee for general technical help especially in NMR data processing.

References

1. Whitman WB, Coleman DC, Wiebe WJ. *Proc Natl Acad Sci USA*. 1998; 95:6578–6583. [PubMed: 9618454]
2. Fenical W. *Chem Rev*. 1993; 93:1673–1683.
3. Blunt JW, Copp BR, Keyzers RA, Munro MHG, Prinsep MR. *Nat Prod Rep*. 2014; 31:160–258. [PubMed: 24389707]
4. Souto A, Montaños MA, Rivas AJ, Balado M, Osorio CR, Rodriguez J, Lemos ML, Jimenez C. *Eur J Org Chem*. 2012; 29:5693–5700.
5. Xu Y, Kersten RD, Nam SJ, Lu L, Al-Suwailem A, Zhenge H, Fenical W, Dorrestein PC, Moore BS, Qian PYJ. *Am Chem Soc*. 2012; 134:8625–8632.
6. Pinhassi J, Zweifel UL, Hagström A. *Appl Environ Microbiol*. 1997; 63:3359–3366. [PubMed: 9292985]
7. Joint I, Muhling M, Querellou J. *Microb Biotechnol*. 2010; 3:564–575. [PubMed: 21255353]
8. Still PC, Johnson TA, Theodore CM, Loveridge ST, Crews P. *J Nat Prod*. 2014; 77:690–702. [PubMed: 24571234]
9. Weissmann KJ, Müller R. *Nat Prod Rep*. 2010; 27:1276–1295. [PubMed: 20520915]
10. König GM, Kehraus S, Seibert SF, Abdel-Lateff A, Müller D. *Chem Bio Chem*. 2006; 7:229–238.
11. Tsukimoto M, Nagaoka M, Shishido Y, Fujimoto J, Nishisaka F, Matsumoto S, Harunari E, Imada C, Matsuzaki T. *J Nat Prod*. 2011; 74:2329–2331. [PubMed: 22035372]
12. Reichenbach, H.; Dworkin, M. *The Prokaryotes*. 2nd. Balows, A.; Trüper, HG.; Dworkin, M.; Harder, W.; Schleifer, KH., editors. Springer-Verlag; Berlin: 1992. p. 3416–3487.
13. Berrue F, Withers ST, Haltli B, Withers J, Kerr RG. *Mar Drugs*. 2011; 9:369–381. [PubMed: 21556166]
14. Wietz M, Mansson M, Gotfredsen CH, Larsen TO, Gram L. *Mar Drugs*. 2010; 8:2946–2960. [PubMed: 21339958]
15. Qin Z, Baker AT, Raab A, Huang S, Wang T, Yu Y, Jaspars M, Secombes CJ, Deng H. *J Biol Chem*. 2013; 288:14688–14697. [PubMed: 23572522]
16. Kenig M, Reading C. *J Antibiot*. 1979; 32:549–554. [PubMed: 468729]

17. de Nys R, Kumar N, Sharara KA, Srinivasan S, Ball G, Kjelleberg S. *J Nat Prod.* 2001; 64:531–532. [PubMed: 11325243]
18. Suzuki A, Goto M. *Biochim Biophys Acta.* 1973; 313:229–234. [PubMed: 4355564]
19. Mansson M, Nielsen A, Kjærulff L, Gotfredsen CH, Wietz M, Ingmer H, Gram L, Larsen TO. *Mar Drugs.* 2011; 9:2537–2552. [PubMed: 22363239]
20. Adachi, K.; Kawabata, Y.; Kasai, H.; Katsuta, M.; Shizuri, Y. Japanese patent JP 2007230911. 2007.
21. Oku N, Kawabata K, Adachi K, Katsuta A, Shizuri Y. *J Antibiot.* 2008; 61:11–17. [PubMed: 18305354]
22. Kjaerulff L, Nielsen A, Mansson M, Gram L, Larsen TO, Ingmer H, Gotfredsen CH. *Mar Drugs.* 2013; 11:5051–5062. [PubMed: 24351904]
23. Stackebrandt E, Goebel BM. *Int J Syst Bacteriol.* 1994; 44:846–849.
24. Rivas R, Garcia-Fraile P, Mateos PF, Martinez-Molina E, Velazquez E. *Int J Sys Evol Microbiol.* 2006; 56:1067–1071.
25. Appleton DR, Buss AD, Butler MS. *Chim Int J Chem.* 2007; 61:327–331.
26. Harrigan GG, Harrigan BL, Davidson BS. *Tetrahedron.* 1997; 53:1577–1582.
27. Yoshitaka, K.; Kenichi, M.; Miyuki, N.; Masato, S. Japanese patent JP2000245497-A 20000912. 2000.
28. Raju R, Kawabata K, Nishijima M, Aalbersberg WGL. *Tetrahedron Lett.* 2012; 53:6905–6907.
29. Fuji K, Ikai Y, Mayumi T, Oka H, Suzuki M, Harada KI. *Anal Chem.* 1997; 69:3346–3352.
30. Crews, P.; Rodríguez, J.; Jaspars, M. *Organic Structure Analysis.* 2nd. Oxford University Press; New York: 2010. p. 82, 152
31. Marfy P. *Carlsberg Res Commun.* 1984; 49:591–596.
32. Hess S, Gustafson KR, Milanowski DJ, Alvira E, Lipton MA, Pannell LKJ. *Chromatogr A.* 2004; 1035:211–219.
33. Rao KV, Na M, Cook JC, Peng J, Matsumoto R, Hamann MT. *J Nat Prod.* 2008; 71:772–778. [PubMed: 18407693]
34. Hashizume H, Hirose S, Sawa R, Muraoka Y, Ikeda D, Naganawa H, Igarashi M. *J Antibiot.* 2004; 57:52–58. [PubMed: 15032486]
35. Wyche TP, Hou Y, Vazquez-Rivera E, Braun D, Bugni TS. *J Nat Prod.* 2012; 75:735–740. [PubMed: 22482367]
36. Lam T, Salvatore MJ, Hirsch C, Hensens OD, Zink D, Bernard-King A, Lee N, Graham A, Pelak B. *Tetrahedron.* 1998; 54:4755–4760.
37. Trischman JA, Jensen PR, Fenical W. *Tetrahedron Lett.* 1994; 35:5571–5574.
38. Dale JA, Mosher HS. *J Am Chem Soc.* 1973; 95:512–519.
39. Su BN, Park EJ, Mwambo ZH, Santarsiero BD, Mesecar AD, Fong HHS, Pezzuto JM, Kinghorn AD. *J Nat Prod.* 2002; 65:1278–1282. [PubMed: 12350147]
40. Seco JM, Quiñoá E, Riguera R. *Chem Rev.* 2004; 104:17–117.
41. Yu HM, Chen ST, Wang KT. *J Org Chem.* 1992; 57:4781–4784.
42. Druais V, Hall MJ, Corsi C, Wendeborn SV, Meyer C, Cossy J. *Org Lett.* 2009; 11:935–938. [PubMed: 19170620]
43. Salit AF, Meyer C, Cossy J, Delouvrie B, Hennequin L. *Tetrahedron.* 2008; 64:6684–6697.
44. Gracia C, Isidro-Llobet A, Cruz LJ, Acosta GA, Alvarez M, Cuevas C, Giralt E, Albericio F. *J Org Chem.* 2006; 71:7196–7204. [PubMed: 16958512]
45. Chatterjee J, Laufer B, Kessler H. *Nat Protoc.* 2012; 7:432–444. [PubMed: 22322216]
46. Subiros-Funosas R, Nieto-Rodríguez L, Jensen KJ, Albericio F. *J Pept Sci.* 2013; 19:408–414. [PubMed: 23712932]
47. Valeriote FA, Tenney K, Media J, Pietraszkiewicz H, Edelstein M, Johnson TA, Amagata T, Crews P. *J Exp Ther Oncol.* 2012; 10:119–134. [PubMed: 23350352]
48. Woehrman MH, Bray WM, Durbin JK, Nisam SC, Michael AK, Glassey E, Stuart JM, Lokey RS. *Mol Biosyst.* 2013; 9:2604–2617. [PubMed: 24056581]
49. Wong WR, Oliver AG, Linington RG. *Chem Biol.* 2012; 16:1583–1495.

50. Enticknap, J.; Hamann, MT.; Hill, RT.; Rao, KVUS. patent WO2005042720A2. 2005.
51. Urbanczyk H, Ogura Y, Hendry TA, Gould AL, Kiwaki N, Atkinson JT, Hayashi T, Dunlap PV. *J Bacteriol.* 2011; 193:3144–3145. [PubMed: 21478348]
52. Park YD, Baik KS, Seong CN, Bae KS, Kim S, Chun J. *Int J Syst Evol Microbiol.* 2006; 56:745–749.
53. Blin K, Medema MH, Kazempour D, Fischbach MA, Breitling R, Takano E, Weber T. *Nucleic Acids Res.* 2013; 41:W240–W212.
54. Iizuka T, Jojima Y, Fudou R, Yamanaka S. *FEMS Microbiol Lett.* 1998; 169:317–322. [PubMed: 9868776]
55. Altschul SF, Gish W, Miller W, Myers EW, Lipman DJ. *J Mol Biol.* 1990; 215:403–410. [PubMed: 2231712]
56. Katoh S. *Mol Biol Evol.* 2013; 30:772–780. [PubMed: 23329690]
57. Saitou N, Nei M. *Mol Biol Evol.* 1987; 4:406–425. [PubMed: 3447015]

**Figure 1.**

A short list of natural products isolated via culturing of marine Gram-negative *Photobacterium* (family Vibrionaceae) strains. Only lead structures are shown, and each is categorized by biosynthetic type as a(n) alkaloid (ALK), polyketide (PK), nonribosomal peptide (NRP), or polyketide–nonribosomal peptide (PK-NRP). Further remarks include additional marine bacteria (coded with ^N for Gram-negative or ^P for Gram-positive) that also produce these exact metabolites in culture.

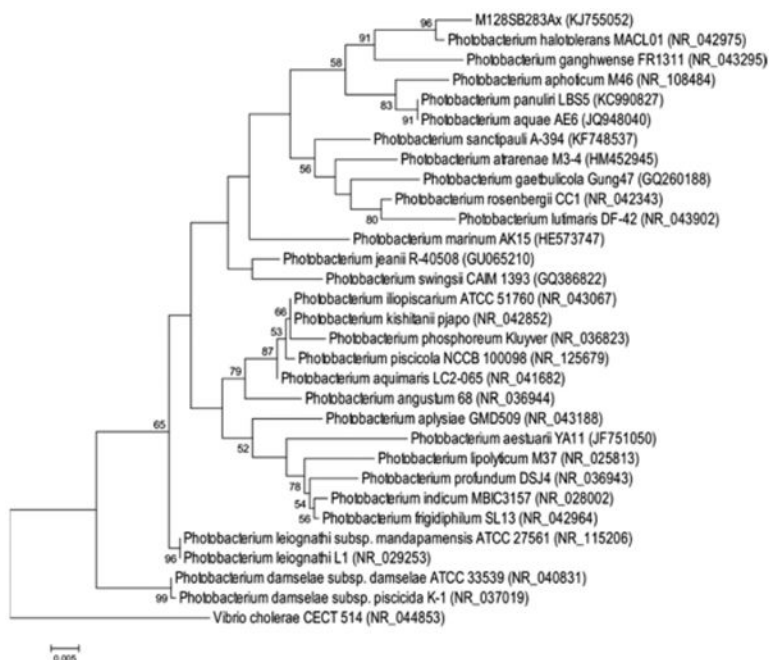
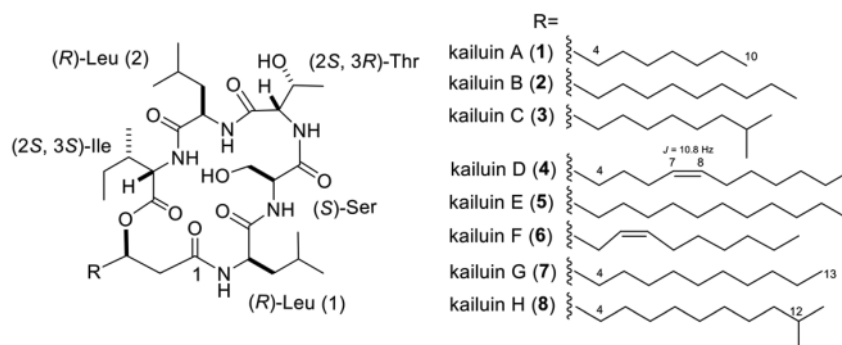


Figure 2.

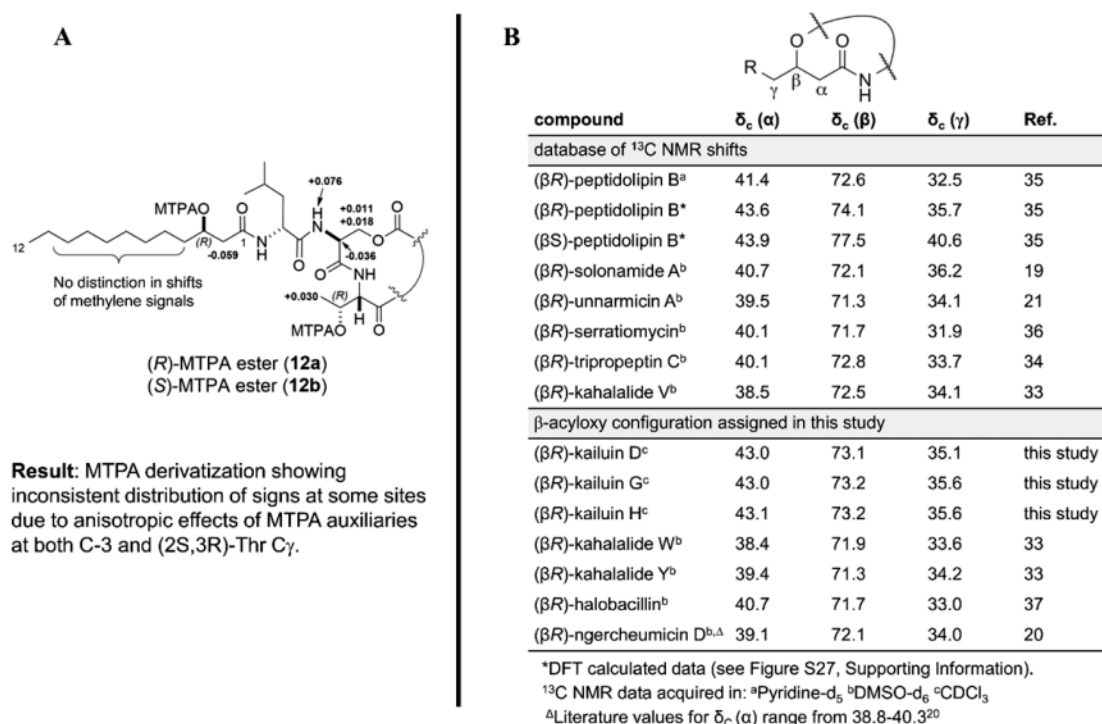
Phylogeny depicted by a maximum likelihood tree constructed in MEGA6 (Molecular Evolutionary Genetics Analysis) from the alignments of 16S rRNA gene sequences. Compared here are (a) UCSC strain M128SB283Ax, which produced compounds **2–5**, **7**, and **8**, (b) 29 representative and/or type strains currently deposited in the NCBI database (accession numbers shown in parentheses), and (c) *Vibrio cholera* used as an outgroup. Bootstrap values >50% are listed for nodes with the scale bar representing 0.005 substitution per position.



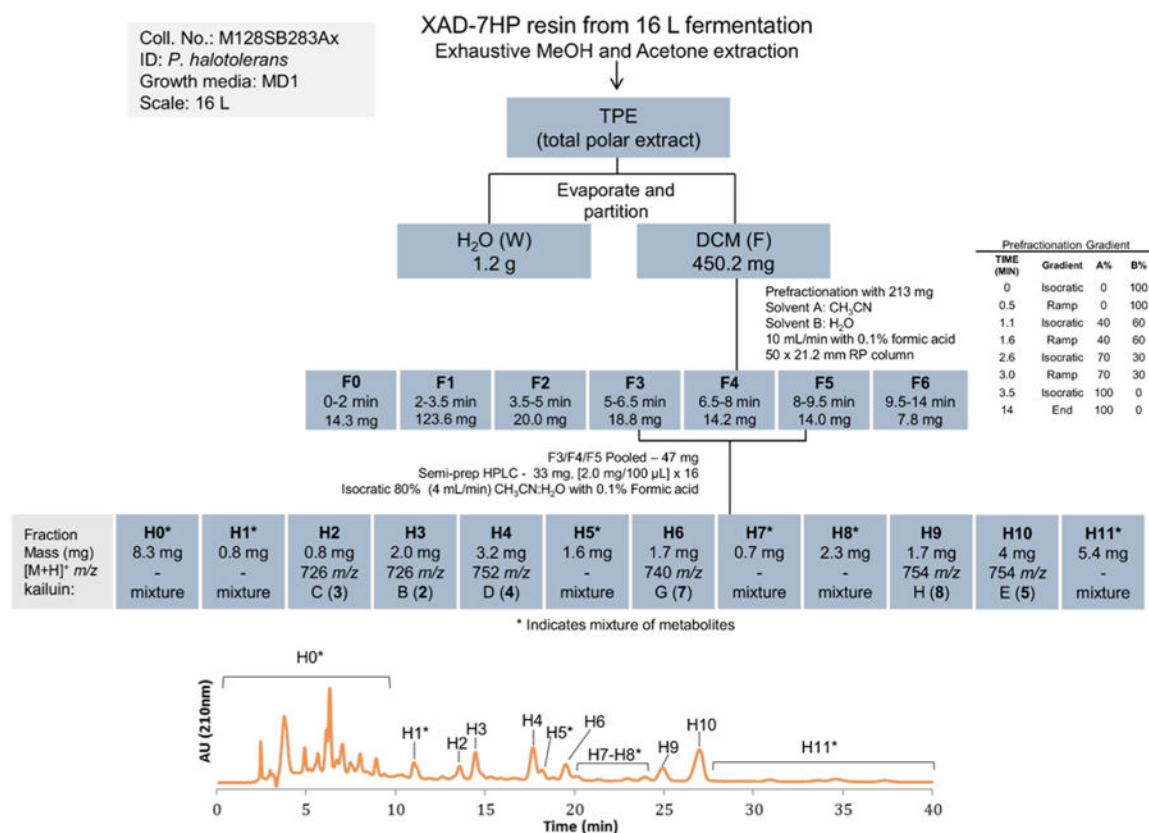
feature	method	compound
amino acid configuration	Marfey's analysis	4, 5
amino acid sequence	^1H , ^{13}C -HMBC	2-5, 7 and 8
configuration at C3	Mosher's reaction	2
	δ_{C} analysis	2-5, 7 and 8

Figure 3.

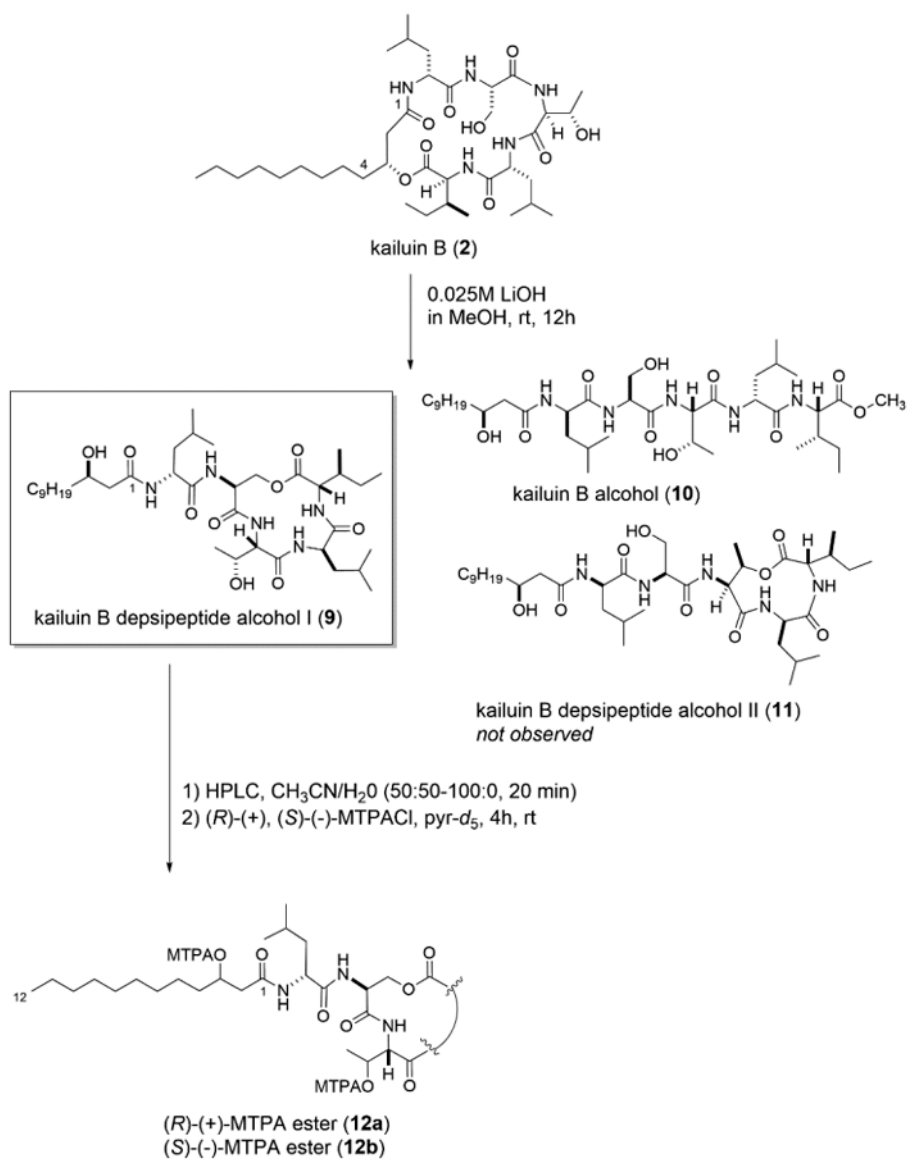
Overview of the kailuin family: known analogues A–F (**1–6**) [with D (**4**) revised] and new members G and H (**7** and **8**). Compounds **2-5**, **7**, and **8** were isolated from *Photobacterium halotolerans* (M128SB283Ax). The coupling constant between protons **7** and **8** is shown to justify double-bond revision for **4**. The *R/S* configurations for the amino acids were determined through Marfey's analysis starting with compounds **4** and **5** (see Figures S25–28, Supporting Information). The configuration at position 3 was determined using two methods: (a) compound **2** as the starting material to prepare compounds **12a/12b** (see Scheme 2), which were evaluated by the Mosher's method ^1H NMR shift analysis (see Figure 4, panel A); (b) analysis of ^{13}C NMR chemical shifts (shown in Figure 4, panel B).

**Figure 4.**

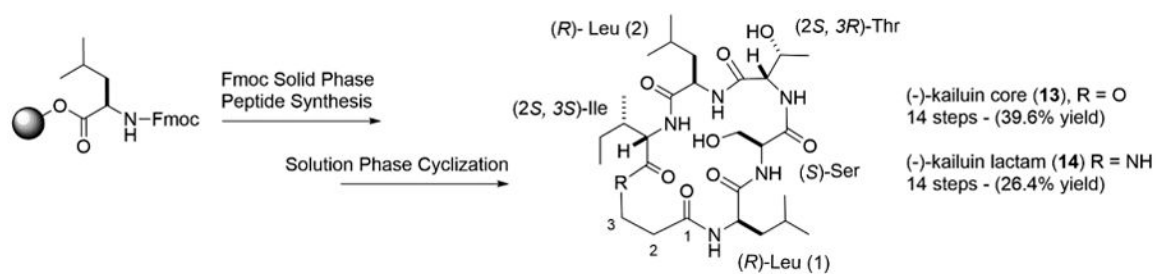
Strategies to assign the β -acyloxy configuration. Panel A shows the δ_{S-R} chemical shift differences measured for (*R*)/(*S*)-MTPA esters (**12a** and **12b**) obtained via the transformations shown in Scheme 2, which employed kailuin B (**2**) as the starting material. The subsequent δ_{S-R} data shown here were used to assign the 3*R*-side chain and the 3*R*-Thr absolute configurations, respectively. Panel B provides, in the upper portion of the table, a database of ^{13}C NMR shifts at three sites proximal to the oxygen center in compounds whose β -acyloxy configuration was assigned in previous studies. The trends in the δ_c at the β and γ are diagnostic of a variation between *R* and *S* and can be used to assign a final configuration at the β -acyloxy position. The lower portion of the table includes compounds whose configurations at the β -acyloxy position were assigned in this study by comparison of the ^{13}C NMR shifts at the β and γ positions to those collected in the database.



Scheme 1. Isolation Scheme of the Six Kailuins (2–5, 7, and 8) from *Photobacterium halotolerans* (M128SB283Ax)



Scheme 2. Summary of the Reaction Products of Kailuoin B (2) Used in the Determination of the Absolute Configurations Justified by the Data Shown in Figure 4, Panel A



Scheme 3. Concise Total Chiral Synthesis of Two Macrolide Analogues: the Kailuin Core (13) and Kailuin Lactam (14).^a

^aDetails on the total synthesis are described in Schemes S1 and S2, Supporting Information.

Table 1

Partial ^{13}C and ^1H NMR Data (125/600 MHz, CDCl_3 , 25°C) for the 3-Hydroxy Acyl Chain for Kailuin D (4)^b and Kailuins G (7)^b and H (8)^b

position	4			7			8		
	δ_{C}	type	δ_{H} , mult (<i>J</i> in Hz)	δ_{C}	type	δ_{H} , mult (<i>J</i> in Hz)	δ_{C}	Type	δ_{H} , mult (<i>J</i> in Hz)
1	171.5	C		171.7	C		171.7	C	
2a	43.0	CH_2	2.47, dd (2.3, 16.4)	43.0	CH_2	2.47, dd (2.1, 16.4)	43.1	CH_2	2.47, dd (2.2, 16.4)
2b			2.54, dd (5.1, 16.4)			2.54, dd (5.1, 16.4)			2.54, dd (5.1, 16.4)
3	73.1	CH	5.06, m ^c	73.2	CH	5.05, m ^c	73.2	CH	5.05, m ^c
4a	35.1	CH_2	1.58, m ^c	35.6	CH_2	1.56, m ^c	35.6	CH_2	1.57, m ^c
4b			1.69, m ^c			1.66, m ^c			1.68, m ^c
5	25.7	CH_2	1.32–1.38, m ^c	25.8	CH_2	1.66, m ^c	25.8	CH_2	1.68, m ^c
6	26.9	CH_2	2.02, q (7.2)	29.8	CH_2	1.45, m ^c	30.1	CH_2	1.46, m ^c
7	128.6	CH^a	5.26, dt (10.8, 7.2)	29.7	CH_2	1.19–1.26, m ^c	29.8	CH_2	1.22–1.26, m ^c
8	131.1	CH^a	5.36, dt (10.8, 7.2)	29.7	CH_2	1.19–1.26, m ^c	29.7	CH_2	1.22–1.26, m ^c
9	27.5	CH_2	1.97, q (7.2)	29.5	CH_2	1.19–1.26, m ^c	29.4	CH_2	1.22–1.26, m ^c
10	29.9	CH_2	1.21–1.31, m ^c	29.5	CH_2	1.19–1.26, m ^c	27.5	CH_2	1.22–1.26, m ^c
11	29.2	CH_2	1.24–1.28, m ^c	32.1	CH_2	1.19–1.26, m ^c	39.2	CH_2	1.11, m ^c
12	32.0	CH_2	1.24, m ^c	23.0	CH_2	1.19–1.26, m ^c	28.2	CH	1.51, m ^c
13	23.0	CH_2	1.27, m ^c	14.3	CH_3	0.85, t (7.2)	22.9	CH_3	0.84, d (6.5)
14	14.3	CH_3	0.86, t (6.9)				22.9	CH_3	0.84, d (6.5)

^aData reported from Harrington et al.²⁶ incorrectly transposed these two assignments.

^bMeasured at 125 MHz in CDCl_3 . For complete NMR data for kailuin D, G, and H (4, 7, 8) see Tables S1 and S2, Supporting Information.

^cOverlapping signals.

Table 2
Summary of Cytotoxicity of the Kailuins against Tumor Cell Lines^a

compound	HCT-116 ^b	MCF-7	
		this study ^b	literature ^c
kailuin A	NT	NT	4
kailuin B	22	NT	3
kailuin C	50	NT	6
kailuin D	28	39	4
kailuin E	18	NT	
kailuin G	32	NT	
kailuin H	17	NT	
kailuin core	>1000	NT	
kailuin lactam	>1000	NT	

^aHuman cancer cell lines: HCT-116 (colon); MCF-7 (breast).

^bIC₅₀ values reported in μ M, calculated based on Valeriote et al.⁴⁷

^cIC₅₀ values reported in μ M, from Harrington et al.²⁶